11-1-2004

SAR and radiation performance of balanced and unbalanced mobile antennas using a hybrid computational electromagnetics

Peter S. Excell
Glyndwr University, p.excell@glyndwr.ac.uk

R A. Abd-Alhameed

R Alias

K Khalil

J Mustafa

Follow this and additional works at: http://epubs.glyndwr.ac.uk/cair

Part of the Digital Communications and Networking Commons, and the Electromagnetics and photonics Commons

SAR and radiation performance of balanced and unbalanced mobile antennas using a hybrid computational electromagnetics

Abstract

The procedure that is required to ensure that the effect of the mobile antenna on the handset can be reduced by using balanced antennas was investigated. However, using this type of antenna may degrade the antenna performance, such as bandwidth and gain, although these antennas can cause less effect on the body to which they are adjacent. Moreover, if these antennas are well-designed, then the maximum specific absorption rate (SAR) values are likely to be reduced when placed next to the human head, since the coupling of such antennas to the body of the handset is very weak. In this paper, a study on balanced and unbalanced antennas for mobile handsets next to the human head is presented, using a hybrid electromagnetic method for the analysis. The method uses the hybridisation technique between the frequency domain Method of Moments (MoM) and the Finite Difference Time Domain method (FDTD). The antenna was modelled using MoM whereas the head tissues were modelled using FDTD. Two antennas were designed and investigated with respect to the SAR and radiation performance for two different antenna positions on the top edge of mobile handsets. Radiation patterns are presented and compared, with and without the human head, and the maximum SAR values and field distribution inside the human head for both antennas are discussed. The balanced antenna shows good improvements with respect to the unbalanced antenna in terms of the SAR values and variations of the input impedances.

SAR AND RADIATION PERFORMANCE OF BALANCED AND UNBALANCED MOBILE ANTENNAS USING A HYBRID COMPUTATIONAL ELECTROMAGNETICS FORMULATION

R.A. Abd-Alhameed, P.S. Excell, K. Khalil, R. Alias and J. Mustafa

Mobile and Satellite Communications Research Centre

Bradford University BD7 1DP, West Yorkshire, UK

Abstract:

The procedure that is required to ensure that the effect of the mobile antenna on the handset can be reduced by using balanced antennas was investigated. However, using this type of antenna may degrade the antenna performance, such as bandwidth and gain, although these antennas can cause less effect on the body to which they are adjacent. Moreover, if these antennas are well-designed, then the maximum specific absorption rate (SAR) values are likely to be reduced when placed next to the human head, since the coupling of such antennas to the body of the handset is very weak. In this paper, a study on balanced and unbalanced antennas for mobile handsets next to the human head is presented, using a hybrid electromagnetic method for the analysis. The method uses the hybridisation technique between the frequency domain Method of Moments (MoM) and the Finite Difference Time Domain method (FDTD). The antenna was modelled using MoM whereas the head tissues were modelled using FDTD. Two antennas were designed and investigated with respect to the SAR and radiation performance for two different antenna positions on the top edge of mobile handsets. Radiation patterns are presented and compared, with and without the human head, and the maximum SAR values and field distribution inside the human head for both antennas are discussed. The balanced antenna shows good improvements with respect to the unbalanced antenna in terms of the SAR values and variations of the input impedances.

Email addresses

r.a.a.abd@bradford.ac.uk

p.excell@glyndwr.ac.uk

SAR AND RADIATION PERFORMANCE OF BALANCED AND UNBALANCED MOBILE ANTENNEAS USING A HYBRID COMPUTATIONAL ELECTROMAGNETICS FORMULATION

R.A. Abd-Alhameed, P.S. Excell, K. Khalil and R Alias

Mobile and Satellite Communications Research Centre, Bradford University, UK

The move toward worldwide wireless communication continues at remarkable pace, and the antenna element of the technology is crucial to its success. Various mobile antenna structures have found increasing attention, significant characteristics being small size and low cost. However, the characteristics also need to be optimised with respect to the antenna radiation patterns and the Specific Absorption Rate (SAR) levels for compliance with international safety guidelines [1,2]. Moreover, the antenna should have weak coupling with the body of the handset to provide the best impedance matching in the presence of a human hand.

A good candidate for this purpose is to use a balanced antenna [3,4]. The antenna can be used on top of the handset [3] or mounted on one side [4]. However, in [4] the SAR distribution and matching were not presented in detail and in [3] the total axial length of the antenna was high because of the existence of the feed balun.

In this paper, some powerful techniques are presented for the design of balanced and unbalanced compact meander-line loop antennas, mounted on the side of the body of the handset, as shown in Fig. 1. The centre operating frequency was chosen as 1800 MHz. The position of the antenna from the top edge of the handset was tested against the performance, using two different distances for each antenna design considered. The antenna was modelled using the frequency-domain Method of

Moments (MoM) and then inserted into the FDTD model using the hybrid technique [5,6], then each antenna's performance was predicted with and without the presence of the human head.

ANTENNA DESIGN CONCEPT AND SUMMARY OF THE METHOD

The body of the handset was represented as a rectangular conducting plate with dimensions 50 mm x 120 mm (i.e. 0.3λ x 0.72λ at f = 1800MHz). The antennas were placed at a distance of 0.027λ to 0.03λ from the surface of the handset. The total area occupied by each antenna was 0.27λ by 0.034λ, in a plane normal to the handset. Several attempts were made to achieve the best matching characteristics by varying the lengths of the meander-line arms inside the area size stated above. However, the total length of the meander was always kept between 0.5λ and λ (free-space wavelength).

The constraints on the antenna designs were, firstly, the free space resonance length required at the operating frequency and, secondly, the total area required to accommodate the antenna inside a typical phone. Subject to these considerations, the design was optimised using trial and error procedures since the degrees of freedom were already tightly constrained. Of the designs shown in Fig. 1, Fig. 1c represents a balanced antenna working at its first resonance. Figs. 1d to 1g are different geometries for unbalanced antennas. Figs. 1d and Fig. 1e are working at their second resonance, while Figs. 1f and 1g are designed to operate at their first resonance. Figs. 1e and 1g are similar to Figs 1d and 1f except they have a wider distance between the input port and the other end of the meander antenna.

Following establishment of the antenna design in the MoM region, each MoM antenna model was placed inside the FDTD domain using an equivalent Huygens surface at the boundary, as shown in

Fig. 2. The details of the method, and specific explanations of the tangential fields (E_b and H_b: the back scattered fields) and surface currents (J and M: the excitation currents) shown in Fig. 2 are given fully in refs. [5,6].

SIMULATION AND RESULTS

The cell size used in the FDTD portion was 2.5 mm (cubes) and the size of the problem space was $127 \times 90 \times 127$ cells. Within this, the Huygens surface size was $36 \times 36 \times 74$ cells. The head model was a realistic head image, taken from an MRI scan of a real human head, and segmented into 13 different tissue types [7]. The exterior of the FDTD region was terminated with a perfectly matched layer 6 cells deep, with a geometric grading factor of 5.34. The computed results with and without the human head are summarised as follows:

The input voltage standing wave ratios (VSWR) versus the frequency, without the human head, are presented in Fig. 3 for the cases: balanced (Fig. 1c); unbalanced at 2nd resonance (Fig. 1d) and unbalanced at 1st resonance (Fig. 1f). These results appear to show better overall matching to 50 ohms over the desired range than was previously reported [4]. The results for the alternative designs with wide feed gaps (Figs 1e and 1g) were within 2% of those for the corresponding versions with narrow feed gaps (not displayed, for clarity). The same was true when the antennas were moved up to the top edge of the handset. The computed value of the maximum current density in the simulated handset with the balanced antenna was between 0.63 and 0.83 of the value with the various unbalanced designs. Moreover, the E_θ component of electric field in the xz-plane for the balanced antenna was found to be very low compared to the same component for the unbalanced antennas. In the xy plane, the computed maximum horizontally-polarised power gains for balanced

and unbalanced antennas were 2.8 dB and 2.5 dB respectively, whereas the vertically-polarised power gains were found to be relatively very low for all antennas.

The near total field along a line parallel to the z-axis, with and without the head, is shown in Fig. 4 for x = 27.75mm, y = 0.0mm, with the antenna in the xy plane and the head placed 6.5mm from the handset in the x-direction. The near fields in the absence of the head were computed using the using both the hybrid technique (with empty FDTD region) and with the pure Method of Moments [5]: excellent agreement is observed, giving a validating benchmark test.

Radiation patterns for balanced and unbalanced antennas (Figs. 1c and 1f), with the head present, are shown in Figs. 5 and 6 respectively. The results for the other designs were similar (within 3dB) to one or the other of these and hence are not presented. The most important point to notice is that, for the balanced antenna, the horizontally-polarised component (E_ϕ) is greater than the vertically-polarised component (E_θ), in most directions, but the reverse is true for the unbalanced antenna: this appears to be due to currents coupled into the handset chassis in the latter case, making the handset a significant vertical radiator. For the balanced antenna, the overall quality of the polarisation can also be said to be more consist (mainly horizontal).

The computed input impedances for balanced, unbalanced (2nd resonance: Fig. 1d) and unbalanced (1st resonance: Fig. 1f) antennas without the head were (24 + j3), (25 – j2) and (38 + j5) ohms respectively, while with the head they were (20 – j4), (18 – j18) and (20 – j22) ohms respectively. The small change in impedance of the balanced antenna indicates that it has lower mutual coupling with the head.

The calculated peak SAR, the maximum averaged SAR over masses of 10g and 1g and the power absorbed, for different distances between the head and the handset, are summarised in Table 1 for an input power of 1W. The results also show the SAR for two different antenna positions from the top edge of the handset, no significant differences being recorded for each antenna. The worst-case SAR distributions in the xy plane (containing the antenna), for balanced and unbalanced (Fig. 1f) antennas are presented in Fig. 7. As shown, the balanced antenna presents lower peak SAR values compared to all of the unbalanced antennas. However, the mass-averaged values give less clear results, the 2nd resonance unbalanced design giving a slightly higher SAR than the balanced design, but the 1st resonance unbalanced design giving the lowest results. For a head-handset separation of 6.5 mm the powers absorbed by both balanced and unbalanced antennas are comparable. Basically, the computations indicate that approximately 29% (balanced) and between 26% and 41% (unbalanced) of the total delivered power was absorbed by the head. These results are lower than those reported in [8] for a GSM 1800 terrestrial handset, for which peak SAR in the head was between 15 and 30W/kg/W for a head-handset separation of 6.5mm. Additionally, the head absorbed between 40 and 60% of the power delivered to the antenna.

CONCLUSIONS:

A new design of compact balanced and unbalanced meander-loop antenna, mounted on the side of a handset and next to the human head, has been presented and analysed using the hybrid MoM/FDTD method. The balanced antennas show less effect on the induced handset currents and the radiation pattern is more consistent. The corresponding computed peak SAR values for the balanced antenna was significantly lower than for the unbalanced antennas, although the averaged SAR values were more convergent. The induced current considerations suggest that the SAR values for the balanced antenna could be further reduced if the feeding port were to be shifted to the centre of the edge of the antenna away from the handset.

References

1. "Evaluating compliance with FCC guidelines for human exposure to radio frequency electromagnetic fields", Federal communication Commission, Washington, DC, OET Bulletin 65, Aug. 1997.

2. ICNIRP Guidelines, "Guidelines for limiting exposure to time-varying electric, magnetic, and electromagnetic fields (up to 300 GHz)", Health Phys., vol. 74, no. 4, pp. 494-522, 1998.

3. O. Leisten, Y. Vardaxoglou, T. Schmid et al, 'Miniature dielectric-loaded personal telephone antennas with low user exposure', Electronics Lett., 1998, 34, (17), pp. 1628-1629.

4. H. Morishita, H. Furuuchi and K. Fujimoto, 'Performance of balanced-fed antenna system for handsets in the vicinity of a human head and hand', IEE Proc. Microw. Antennas Propag., vol. 149, No. 2, April 2002, pp. 85-91.

5. M.A. Mangoud, R.A. Abd-Alhameed and P.S. Excell, 'Simulation of human interaction with mobile telephones using hybrid techniques over coupled domains', IEEE Trans. Microwave Theory and Techniques, Vol. 48, No. 11, pp. 2014-2021, Nov. 2000.

6. Mangoud, M.A., Abd-Alhameed, R.A., Excell, P.S. & Vaul, J.A.: 'Conduction current crossing domain boundaries in heterogeneous hybrid computational electromagnetics formulation', Electron. Lett., Vol. 35, No. 21, pp. 1786-1788, Oct. 1999.

7. P.S. Excell, 1998, 'Computer modelling of high frequency electromagnetic field penetration into the human head', *Measurement and Control,* Vol.31, No.6, 170-175.

8. K. S. Nikita, M Cavagnaro, and et al., "A study of uncertainties in modelling antenna performance and power absorption in the head of a cellular phone user", IEEE Trans on MTT, vol. 48, No. 12, Dec. 2000, pp. 2676-2685.

List of figures and tables:

Table 1. SAR and power absorbed for various distances between the head and the handset; (H) distance between head and handset plane in mm; (UNSAR) max unaveraged SAR in W/kg; (AVSAR1GM) max. averaged SAR over 1g (W/kg); (AVSAR10GM) max. averaged SAR over 10g (W/kg); (POWABS) Power absorbed in mW; P1 and P2: the antenna is placed at 1cm and 0cm from the top edge of the handset respectively.

Figure 1. Configurations studied. (a): Balanced meander loop antenna with conducting plate; (b): Unbalanced antenna with conducting plate; (c): Balanced antenna design; (d): Unbalanced antenna design for second resonance with feed width $w = 0.06\lambda$; (e): Unbalanced antenna for second resonance with $w = 0.18\lambda$; (f): Unbalanced antenna for first resonance with $w = 0.06\lambda$; (g): Unbalanced antenna for first resonance with $w = 0.18\lambda$. (w is the width between the feed port and the other end of the antenna). Note that, in Figs 1a and 1b, the plate simulating the handset is in the plane $x = 0$ and the antennas are in the plane $z = 0$; the origin of co-ordinates is at the centre of the intersecting line.

Figure 2. Hybrid MoM/FDTD configuration for a single source and scatterer geometries.

Figure 3. VSWR versus the frequency: —— balanced (Fig. 1c); - - - - unbalanced, 2nd resonance (Fig. 1d); $\cdots$ unbalanced, 1st resonance (Fig. 1f).

Figure 4. Total near field distribution along a line passing through the head region using the hybrid technique (compared with pure MoM for the head-absent case).
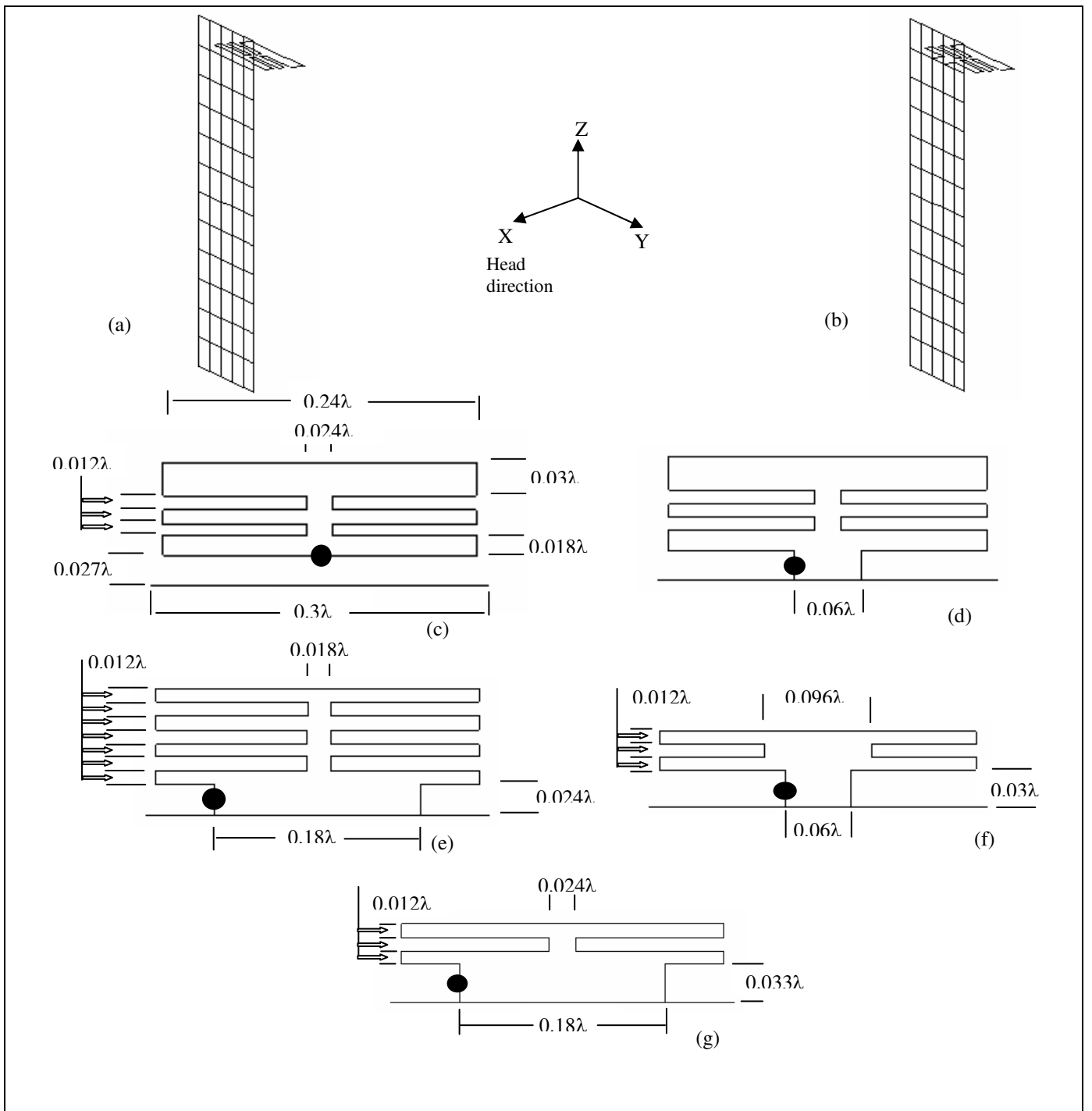
Figure 5. E_θ (ooo) and E_ϕ (xxx) in dB for 1 watt input power versus (a) ϕ at $\theta = 90°$; (b) θ at $\phi = 0°$; for balanced antenna (Fig. 1c).

Figure 6. E_θ (ooo) and E_ϕ (xxx) in dB for 1 watt input power versus (a) ϕ at $\theta = 90°$ (b) θ at $\phi = 0°$; for unbalanced antenna (Fig. 1f).
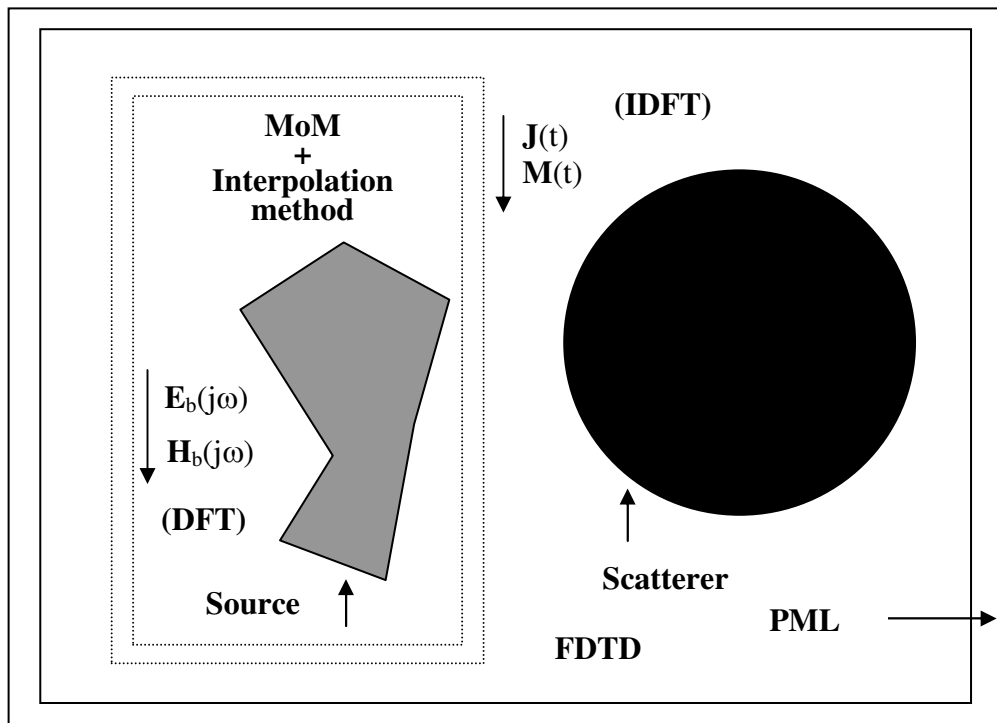
Figure 7. SAR distribution (in dB for 1 watt input power) for horizontal slice containing maximum;

(a) balanced antenna; (b) unbalanced antenna shown in Fig. 1f.

Table 1.

H	Computed parameters	Balanced Fig. 1c		Unbalanced Fig. 1e		Unbalanced Fig. 1g	Unbalanced Fig. 1d		Unbalanced Fig. 1f	
		P1	P2	P1	P2	P1	P1	P2	P1	P2
6.5	UNSAR	9.4	12.24	12.28	14.86	13.05	27.68	33.05	27.37	33.00
	AVSAR1GM	4.43	4.66	5.64	5.55	5.87	2.01	3.85	2.04	3.74
	AVSAR10GM	3.2	3.58	4.16	4.24	4.27	1.55	2.87	1.55	2.74
	POWABS	295	357	386	410	350	260	312	253	302
10	UNSAR	6.33		8.37			21.85			
	AVSAR1GM	3.05		3.86			1.62			
	AVSAR10GM	2.26		2.88			1.24			
	POWABS	242		304			228			
15	UNSAR	4.63		5.91			18.22			
	AVSAR1GM	2.26		2.72			1.31			
	AVSAR10GM	1.69		2.04			1.01			
	POWABS	205		243			199			
20	UNSAR	3.74		4.33			15.04			
	AVSAR1GM	1.74		1.99			1.14			
	AVSAR10GM	1.31		1.51			0.87			
	POWABS	179		202			174			

Fig. 1.

MoM
+
Interpolation
method

(IDFT)

$\mathbf{J}(t)$
$\mathbf{M}(t)$

$\mathbf{E}_b(j\omega)$

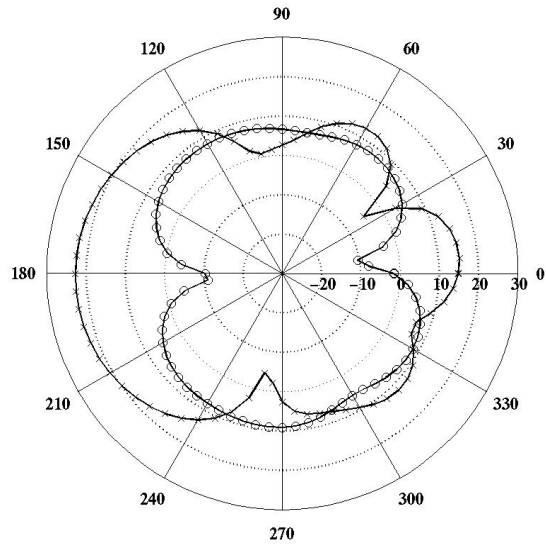$\mathbf{H}_b(j\omega)$

(DFT)
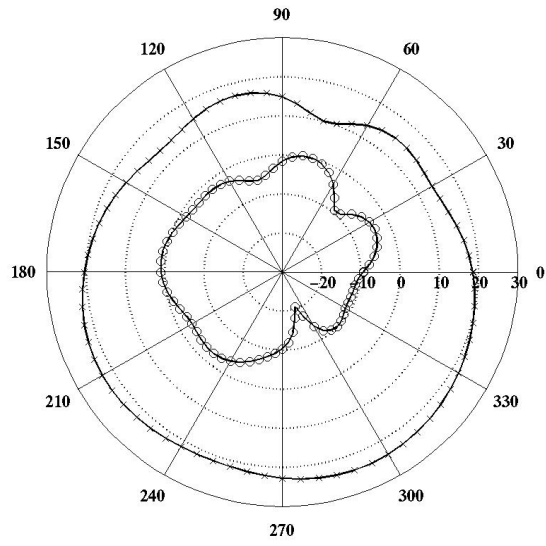
Source

Scatterer
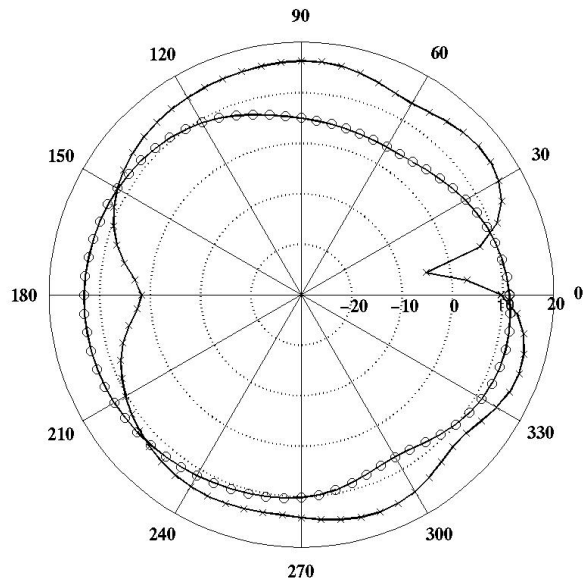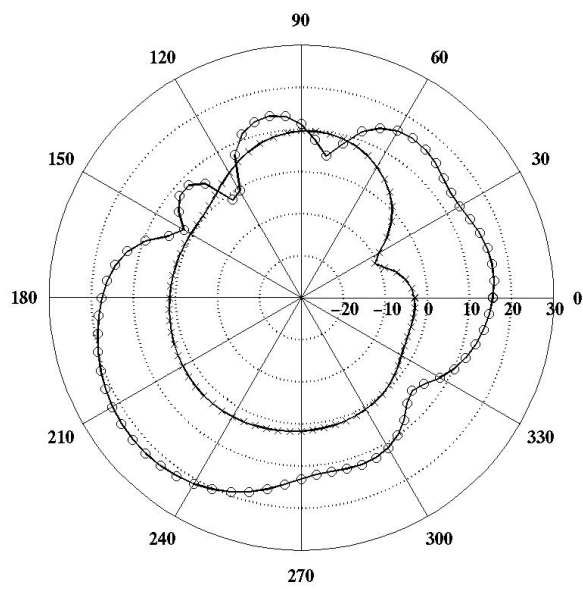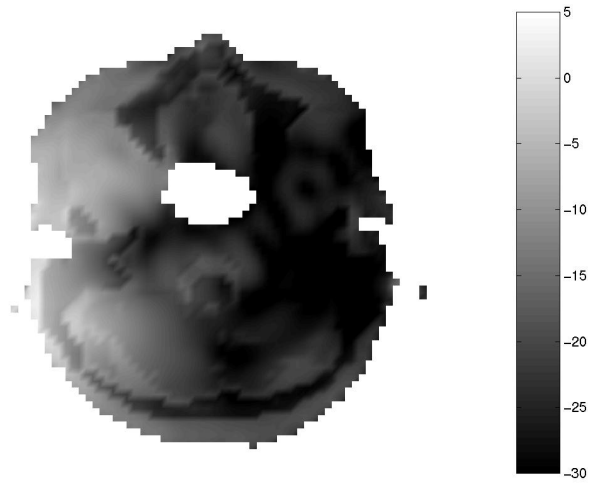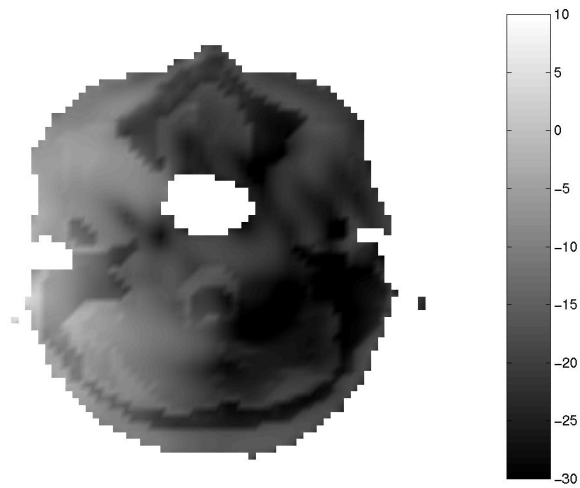
PML

FDTD

Fig. 2.
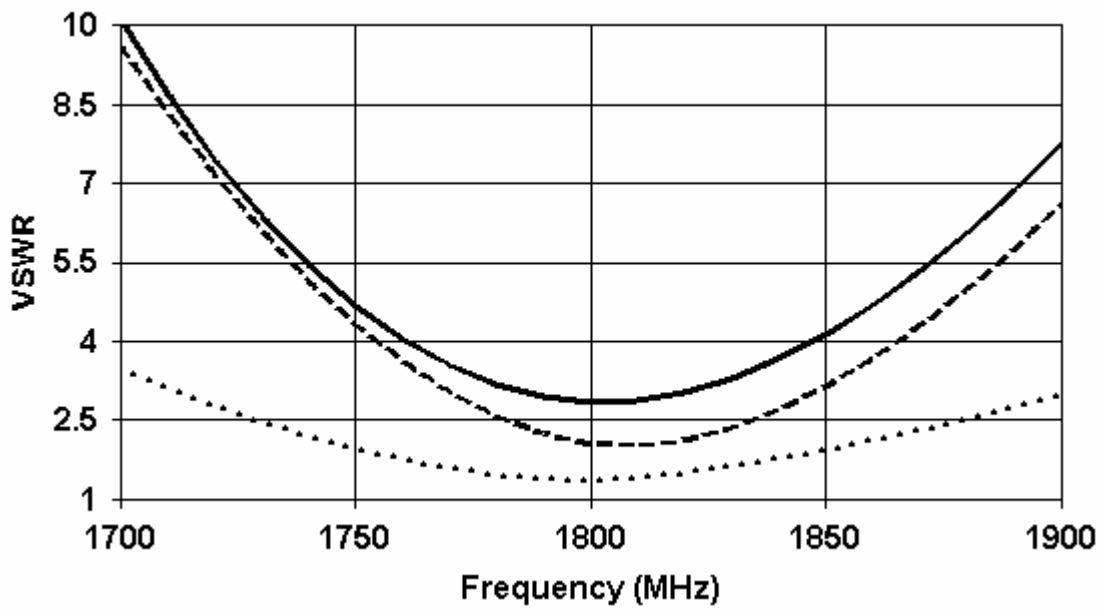
Fig. 3
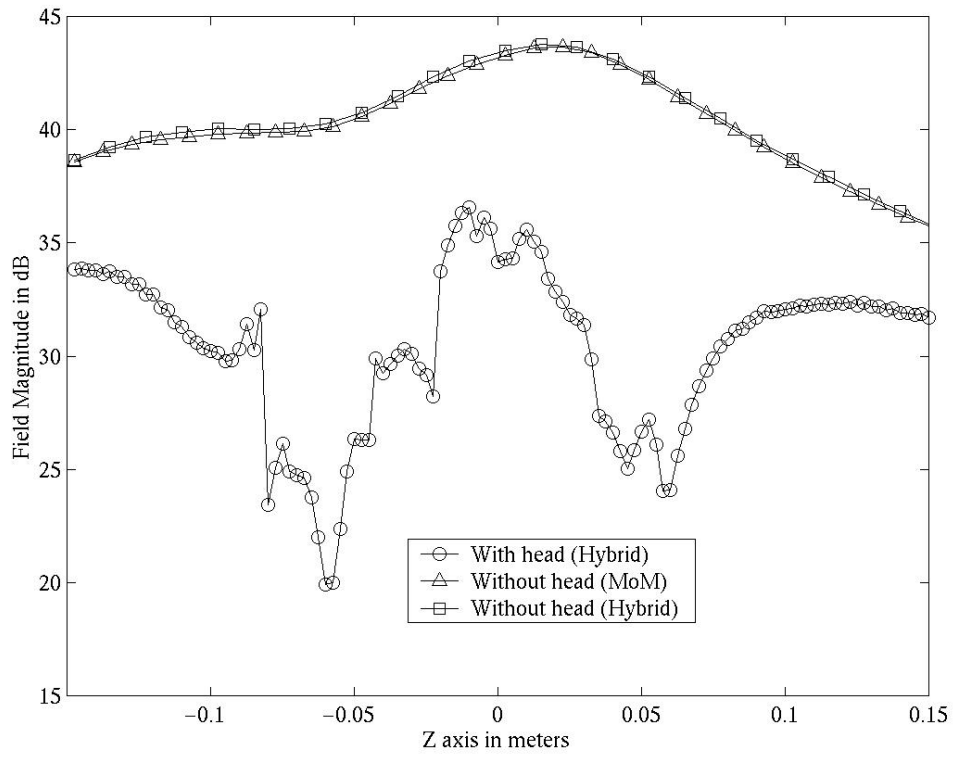
Fig. 4.

(a)

(b)

Fig. 5

(a)

(b)

Fig. 6

(a)

(b)

Fig. 7